

PERFORMANCE SIMULATION OF FLUIDIZED-BED COAL COMBUSTORS

Ravi R. Chandran and Denny D. Sutherland

The Babcock & Wilcox Company, R&D Division, Alliance, Ohio 44601

ABSTRACT

A code, referred to as FBCSIM, is being developed to predict large-scale atmospheric fluidized-bed combustor (AFBC) performance with fundamental fuel data from bench-scale test units as input. This work is carried out as a part of AFBC fuels characterization program sponsored by the Electric Power Research Institute (EPRI). The code accounts for the physics of fluidization, which is unit specific, and the chemistry of combustion, which is fuel specific. The code includes a 3-D model and modules on bed hydrodynamics, chemical kinetics, solid distribution, and transport phenomena. The model for in-bed combustion incorporates a two-region particle mixing formulation. The code for in-bed combustion has been validated for different AFBC unit sizes (0.1, 2, and 20 MW) and different coals (two bituminous and a lignite). Sensitivity analyses have been carried out to identify the controlling variables and guide experimental work. Computer simulations have also been performed to delineate system response to operational parameters.

INTRODUCTION

Test results from small-scale to pilot plant AFBC units have proven the viability of fluidized-bed combustion technology for large-scale applications. However, commercialization of this technology has been slow due in part to concerns regarding scale-up for unit size and fuel type. To overcome this hurdle, Babcock & Wilcox (B&W) under the sponsorship of EPRI has developed an AFBC fuels characterization method (1)(2). The approach involves the generation of fundamental fuel data using inexpensive bench-scale tests and the development of a mathematical model or performance code to link bench-scale results to large-scale operation. The objectives are to 1) facilitate the optimal design of commercial-size AFBC units, and 2) quantify the fuel flexibility of existing AFBC designs. For a review of the models reported in the literature along with the rationale for the present model, the reader is referred to an earlier publication (3).

FORMULATION

The performance code (FBCSIM) under development for bubbling-bed combustion comprises a model and four modules, and has been set up in this fashion so that it is easily adaptable to circulating as well as pressurized FBC. The first module evaluates hydrodynamics, which is unit specific. It accounts for fluidization regime, gas flow, bubble dynamics, and solids mixing characteristics. The second module deals with chemical kinetics (devolatilization, char combustion, and sorbent sulfation), which is influenced by coal and sorbent properties. The third module accounts for solids distribution in bed and above bed due to swelling, fragmentation, attrition, elutriation, and entrainment. The fourth module deals with transport phenomena such as interphase heat and mass transfer. For a given coal and specified operating conditions, the code seeks to predict overall combustion and sulfur capture efficiencies and combustion split and sulfur capture split between in-bed and freeboard. The first goal of this code development was to model in-bed combustion for the underbed-feed mode of operation. Additional goals are to model freeboard combustion, overbed-feed mode, and sulfur capture. The in-bed combustion model is described here.

Model for In-Bed Combustion

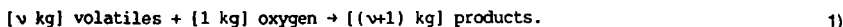
The in-bed combustion model currently addresses underbed feed with zero recycle. Future modifications will account for recycle. Figure 1 shows an idealization of the combustion sequence, and Figure 2 shows the corresponding conceptual model. The figures depict a unit cell defined as the bed cross section served by one feedpoint. Primary air enters the bed through a distributor plate, while coal particles of a broad size distribution (typically 6.35 mm x 0, or 1/4 inch x 0) and transport air enter through the feedpoint. Based on a review of the pertinent physical and chemical time scales, it is suggested that these coal particles entering the bed be classified in a binary fashion for modeling volatile release and heterogeneous combustion. Material below the maximum elutriable size for the given operating conditions is termed "fines" and the larger size fraction is denoted as "coarse". For example, at typical AFBC operating conditions, the fines would correspond to material passing through 30 sieve (590 microns).

The solids injected through the feedpoint flow up through the bed and diffuse laterally. The fines are considered to be in plug flow. They heat up, devolatilize, and burn while convecting axially and dispersing radially until they reach the bed surface and elutriate. The coarse particles also heat up and devolatilize as they mix above the feedpoint. If the coal contains a significant proportion of volatiles, a volatile-rich zone above the feedpoint could result. The volatiles released would rise as a plume and burn in a gaseous diffusion flame with the surrounding oxygen. Whether this plume closes within the bed or not would depend on the coal's ratio of volatile to fixed carbon, feedpoint spacing, and the bed operating conditions. Some coarse particles could fragment during devolatilization if their size exceeds the critical stable size for fragmentation. The coarse char particles mix in the bed, generate flakes and fines due to combustion-enhanced mechanical attrition (CEMA), and combust in the oxidizing zone outside the plume until they reach the elutriable size. The flakes and fines resulting from CEMA are subject to the competing processes of combustion in the bed and elutriation to the freeboard. Therefore, feedpoint spacing has different implications for different coal ranks with regard to in-bed combustion. For low volatile coals or other solid fuels, the wider the feedpoint spacing, the lower the combustion of fines in the feed due to high concentration of fuel and low concentration of oxygen above the feedpoint. For high volatile coals, the occurrence of a volatile-rich plume additionally could diminish in-bed combustion. A video of the bed surface taken recently during 0.1 MW AFBC operation supports the conceptual model discussed above.

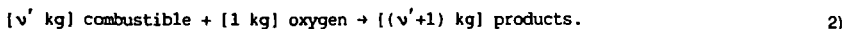
To model in-bed combustion, it is necessary to properly account for the combustion of volatiles, devolatilized fines in the feed, and coarse char particles. These three components burn in a coupled fashion and the degree of combustion is governed by fluidization physics and fuel chemistry. The underlying physical and chemical processes are complex and not fully understood. Therefore, some simplifying assumptions have been introduced (3). Consequently, combustion is visualized to occur in two regions. The first region is where the physical processes of convection and dispersion of coal particles are important. This region lies directly above the feedpoint and provides the setting for coal particle heat up, volatile release, volatile combustion, and the combustion of fines in the feed. Although swelling and fragmentation could occur in this region, they do not involve an oxidation step and need not be considered here. The second region includes the whole unit cell, where the coarse char particles are uniformly distributed and undergo heterogeneous combustion in the oxidizing zone outside the plume. The unit cell coordinate geometry for the 3-D formulation is shown in Figure 3.

Considerable attrition occurs in underbed feed systems (1)(2). A distributed fracture model along with an experimentally determined coal-specific attrition parameter are used to estimate the coal particle size distribution $F_i(\bar{d}_i)$ entering the bed.

Region I. The formulation here corresponds to an adaptation of the model of Bywater (4). Five conservation equations are used to designate the problem. These are for the concentration of i) volatiles remaining in the coarse coal particles (C_{Vc}), ii) volatiles remaining in the fines (C_{Vf}), iii) solid combustibles in the devolatilized fines (C_{cf}), iv) gaseous volatiles (C_g), and v) oxygen (C_o). The gaseous volatiles are assumed to combust according to the stoichiometric reaction,



Also the fast reaction or large Damkohler limit is presumed to apply. The heterogeneous combustion of devolatilized fines is considered to follow the reaction,



The reaction order in oxygen is taken to be 0.6 based on the work of Daw (5). Finally, the classical treatment of Burke and Schumann (6) is applied to the combustion of gaseous volatiles. This facilitates the description of a new variable,

$$C_{g0} = C_g - \nu C_o, \quad (3)$$

and reduces the number of variables (and equations) by one.

The mass balance equations are normalized by defining the following variables:

$$x^* = \frac{x}{x_b}, y^* = \frac{y}{y_b}, z^* = \frac{z}{H'}, x_f^* = \frac{x_f}{x_b}, x_o^* = \frac{x_o}{x_b}, y_f^* = \frac{y_f}{y_b}, y_o^* = \frac{y_o}{y_b}$$

$$C_{vc}^* = \frac{C_{vc}}{C_{vci}}, C_{vf}^* = \frac{C_{vf}}{C_{vfi}}, C_{cf}^* = \frac{C_{cf}}{C_{cfi}}, C_{go}^* = \frac{C_{go}}{C_{goi}}$$

where subscript i denotes the parameter value at feedpoint or distributor, x_b and y_b are the length and width of the unit cell, and H' is the bed plus splash zone height.

The governing equations in dimensionless form are:

$$\frac{\partial C_{vc}^*}{\partial z^*} = \alpha_x \frac{\partial^2 C_{vc}^*}{\partial x^{*2}} + \alpha_y \frac{\partial^2 C_{vc}^*}{\partial y^{*2}} - k_{vc}^* C_{vc}^* J_c, \quad 4)$$

$$\frac{\partial C_{vf}^*}{\partial z^*} = \beta_x \frac{\partial^2 C_{vf}^*}{\partial x^{*2}} + \beta_y \frac{\partial^2 C_{vf}^*}{\partial y^{*2}} - k_{vf}^* C_{vf}^* J_f, \quad 5)$$

$$\frac{\partial C_{cf}^*}{\partial z^*} = \beta_x \frac{\partial^2 C_{cf}^*}{\partial x^{*2}} + \beta_y \frac{\partial^2 C_{cf}^*}{\partial y^{*2}} - k_{cf}^* C_{cf}^* (-C_{go}^*)^{0.6} LI, \text{ and} \quad 6)$$

$$\frac{\partial C_{go}^*}{\partial z^*} = \eta_x \frac{\partial^2 C_{go}^*}{\partial x^{*2}} + \eta_y \frac{\partial^2 C_{go}^*}{\partial y^{*2}} + \frac{k_{cf}^* C_{cf}^* (-C_{go}^*)^{0.6} LI \psi \nu R_{fi}}{\nu} + k_{vc}^* C_{vc}^* J_c \phi + k_{vf}^* C_{vf}^* J_f \psi - k_{oc}^* C_{go}^* I, \quad 7)$$

where

$$J_c = \begin{cases} 0 & \text{if } (z^* H' / u_{sc} - \tau_c) \leq 0 \\ 1 & \text{if } (z^* H' / u_{sc} - \tau_c) > 0 \end{cases} \quad J_f = \begin{cases} 0 & \text{if } (z^* H' / u_{sf} - \tau_f) \leq 0 \\ 1 & \text{if } (z^* H' / u_{sf} - \tau_f) > 0 \end{cases}$$

$$L = \begin{cases} 0 & \text{if } C_{vf}^* > 0 \\ 1 & \text{if } C_{vf}^* = 0, \end{cases} \quad I = \begin{cases} 0 & \text{if } C_{go}^* \geq 0 \\ 1 & \text{if } C_{go}^* < 0 \end{cases}$$

Subject to the boundary conditions:

$$\text{at } z^* = 0: \left. \begin{array}{l} C_{vc}^*(x^*, y^*, 0) \\ C_{vf}^*(x^*, y^*, 0) \\ C_{cf}^*(x^*, y^*, 0) \\ C_{go}^*(x^*, y^*, 0) \end{array} \right\} = \begin{cases} 1 & \text{for } x_f^* - \frac{x_o^*}{2} \leq x^* \leq x_f^* + \frac{x_o^*}{2}, y_f^* - \frac{y_o^*}{2} \leq y^* \leq y_f^* + \frac{y_o^*}{2} \\ 0 & \text{for } 0 \leq x^* < x_f^* - \frac{x_o^*}{2}, x_f^* + \frac{x_o^*}{2} < x^* \leq 1, \\ & 0 \leq y^* < y_f^* - \frac{y_o^*}{2}, y_f^* + \frac{y_o^*}{2} < y^* \leq 1 \\ -1 & \text{for } 0 < x^* \leq 1, 0 < y^* \leq 1 \end{cases}$$

$$\text{for } z^* > 1: \quad \frac{\partial C_{vc}^*}{\partial x^*}, \frac{\partial C_{vf}^*}{\partial x^*}, \frac{\partial C_{cf}^*}{\partial x^*}, \frac{\partial C_{go}^*}{\partial x^*} = 0 \text{ at } x^* = 0, 1$$

$$\frac{\partial C_{vc}^*}{\partial y^*}, \frac{\partial C_{vf}^*}{\partial y^*}, \frac{\partial C_{cf}^*}{\partial y^*}, \frac{\partial C_{go}^*}{\partial y^*} = 0 \text{ at } y^* = 0, 1$$

α , β and η are dimensionless dispersion coefficients, k_{vc}^* and k_{vf}^* are normalized devolatilization rate constants, k_{cf}^* is a non-dimensional rate constant for oxidation of combustibles in devolatilized fines, ϕ and ψ are dimensionless solid to gas flux transfer parameters, R_{fj} is the ratio of C_{cfj} and C_{vfj} at the feedpoint, and k_{oc}^* is a normalized reaction rate constant for the depletion of oxygen in the bed due to coarse char particle combustion.

The parameter J accounts for the effect of finite heating rate and the consequent delay in the onset of volatile evolution. It activates the volatile generation term when the particles have convected a distance that corresponds to the heatup time τ . L and l are off/on switching parameters for the heterogeneous combustion of devolatilized fines and coarse char particles respectively. Equations 6 and 7 are coupled through the fines heterogeneous combustion term and hence need to be solved simultaneously. Finally, the last term in equation 7 requires a trial and error procedure to match the coarse char particle combustion occurring in Region II.

Region II. The objective here is to determine the rates of oxygen consumption and elutriation due to the heterogeneous combustion of coarse char particles. This can be accomplished by carrying out solids population balances of the type proposed by Levenspiel, et al. (7)(8).

The flow rates pertaining to the different steps of the combustion sequence are shown in Figure 4. Sorbent and ash particles are assumed to be inert for this analysis. Coarse coal particles represented by $(n-m)$ cut sizes undergo devolatilization. The inflow rate of cut i with mean diameter \bar{d}_i is denoted as $F_i(\bar{d}_i)$. To simplify the analysis, swelling is decoupled from devolatilization. A differential mass balance for the devolatilization step yields:

$$F_w(\bar{d}_i) = (1 - v_i) F_i(\bar{d}_i) \text{ for } i = m+1, m+2, \dots, n, \quad (8)$$

where v_i is the gaseous volatile yield fraction for the i th cut.

Size as well as density change during swelling. Therefore, a number balance rather than a mass balance is indicated. The number flow rate before swelling is related to the mass flow rate according to:

$$N_w(\bar{d}_i) = F_w(\bar{d}_i) / (\rho_{wi} \pi \bar{d}_i^3 / 6) \quad (9)$$

with $\rho_{wi} = \rho_{coal}(1 - v_i)$ and ρ_{coal} is coal density.

From a steady state number balance, the number flow rate after swelling is:

$$N_f(\bar{d}_i) = N_w(\bar{d}_{i-1})(SI_{i-1}-1) \frac{\bar{d}_{i-1}}{\bar{d}_i - \bar{d}_{i-1}} + N_w(\bar{d}_i) \left[1 - (SI_i-1) \frac{\bar{d}_i}{\bar{d}_{i+1} - \bar{d}_i} \right] \quad (10)$$

for $i = m+1, m+2, \dots, n$,

with $N_w(\bar{d}_m) = 0$. SI_i is the swelling index for the i th cut size.

The corresponding mass flow rate is:

$$F_f(\bar{d}_i) = N_f(\bar{d}_i) \rho_{fi} (\pi \bar{d}_i^3 / 6) \text{ for } i = m+1, m+2, \dots, n, \quad (11)$$

where $\rho_{fi} = \rho_{wi} / S I_i^3$.

For typical underbed feed sizes (6.35 mm x 0, or 1/4 inch x 0, experimental data indicates fragmentation to be negligible, therefore,

$$F_C(\bar{d}_i) = F_F(\bar{d}_i) \text{ for } i = m+1, m+2, \dots, n, \quad (12)$$

and

$$\rho_{ci} = \rho_{fi}.$$

The model for char combustion would depend upon coal properties and is likely to correspond to either shrinking size or shrinking core kinetics. Bench-scale experimental data suggest that a shrinking particle model would be a reasonable approximation for bituminous coals. A solids population balance carried out with the modification suggested by Overturf and Kayihan (9) for discrete cut sizes gives:

$$W_C(\bar{d}_i) = \frac{[F_C(\bar{d}_i) - F_{bd}(\bar{d}_i)] \Delta d_i + W_C(\bar{d}_{i+1}) S_C(\bar{d}_{i+1}) \Delta d_i / \Delta d_{i+1}}{S_C(\bar{d}_i) + E_C(\bar{d}_i) \Delta d_i + 3S_C(\bar{d}_i) \Delta d_i / \bar{d}_i} \quad (13)$$

for $i = n, n-1, \dots, (m+1), m$,

with $W_C(\bar{d}_{n+1}) = 0$ and $F_C(\bar{d}_m) = 0$. $W_C(\bar{d}_i)$ is weight of char particles of size \bar{d}_i in bed and Δd_i is size interval for i th cut. Tests in the 1-x 1-foot (1 x 1) and 6-x 6-foot (6 x 6) AFBC units at B&W indicate that the char content of the bed drain solids is very small, therefore,

$$F_{bd}(\bar{d}_i) = 0 \text{ for } i = n, n-1, \dots, (m+1), m. \quad (14)$$

$E_C(\bar{d}_i)$ denotes entrainment rate constant of char particles of size \bar{d}_i from the bed surface. The overall shrinkage rate $S_C(\bar{d}_i)$ is expressed as the sum of the shrinkage rates due to combustion and attrition (10)(11):

$$S_C(\bar{d}_i) = S_{cc}(\bar{d}_i) + S_{ca}(\bar{d}_i). \quad (15)$$

Attrition rate here corresponds to the flakes and fines generated in the CEMA tests. The shrinkage rate for char combustion according to a first order reaction is:

$$S_{cc}(\bar{d}_i) = - \frac{d\bar{d}_i}{dt} \Big|_{cc} = \frac{2 \bar{C}_{ob}}{\rho_{ci} f_{cci} \left[\frac{1}{\lambda_i R_{mc}} + \frac{1}{R_{cc}} \right]} \quad (16)$$

where \bar{C}_{ob} is the mean oxygen concentration in the bed, f_{cci} is the weight fraction of equivalent carbon in char, R_{mc} is the external mass transfer coefficient, and R_{cc} is the chemical rate coefficient for char combustion. λ_i is a parameter that depends on stoichiometry and has a value between 3/8 for $C + O_2 \rightarrow CO_2$ reaction at the char surface and 3/4 for $C + 1/2 O_2 \rightarrow CO$ reaction.

The shrinkage rate due to attrition $S_{ca}(\bar{d}_i)$ is:

$$S_{ca}(\bar{d}_i) = k_{ca} (u_o - u_{mf}) / (3 f_{cci}), \quad (17)$$

where k_{ca} is CEMA rate constant for carbon, u_o is superficial gas velocity, and u_{mf} is the superficial gas velocity at minimum fluidization.

The flakes and fines generated due to CEMA seem to follow the Rosin-Rammler distribution. If q_{ij} and q_{nj} are the weight fraction of flakes and fines of size \bar{d}_j , and f_{fl} is the proportion of flakes in the attrited material, then the weight of char particles of size \bar{d}_j by mass balance is:

$$w_c(\bar{d}_j) = \frac{\sum_{i=m}^n w_c(\bar{d}_i) s_{ca}(\bar{d}_i) [q_{1j} f_{f1} + q_{nj} (1-f_{f1})] \frac{\Delta d_j}{\Delta d_i} + w_c(\bar{d}_{j+1}) s_{cc}(\bar{d}_{j+1}) \frac{\Delta d_j}{\Delta d_{j+1}}}{s_{cc}(\bar{d}_j) + E_c(\bar{d}_j) \Delta d_j + 3 s_{cc}(\bar{d}_j) \Delta d_j / \bar{d}_j} \quad (18)$$

for $j = m-1, m-2, \dots, 1.$

The shrinkage rate S_{cc} depends upon \bar{C}_{ob} , the mean oxygen concentration in the bed which is not known a priori. So the procedure is to start with a guess value of \bar{C}_{ob} and iterate in conjunction with Region I model until convergence. The flow chart for the computer code is given in Figure 5. Subroutines are listed within quotation marks. "FSATT" accounts for feed system attrition, "HYDRO" for bed hydrodynamics, "SOLDIS" for solids distribution, and "CHEMK" for chemical kinetics. "TRANSP" provides interphase heat and mass transfer coefficients and "TEMP" evaluates burning char particle temperature by energy balance. The code is written in FORTRAN and makes use of ACM Algorithm #565, PDETWO/PSETM/GEARB, for solving partial differential equations. Run times for in-bed performance simulations typically range from 2-6 CPU minutes on a DEC VAX 11/785.

To conserve space, the ensuing discussion will be qualitative and will not include equations. From the bed char weight distributions determined above, the rate of oxygen consumption due to char combustion (w_{occl}), char elutriation rate from the bed and the conversion of char in the bed (X_c) are evaluated. It is assumed that any volatiles remaining in the coarse coal particles when they reach the bed surface (based on the solution of Equation 4) are released uniformly in the bed. The oxygen consumption rate due to this component is added to w_{occl} to calculate the overall rate of oxygen consumption in Region II (w_{ocli}).

By integrating the bed-surface concentrations computed in Region I, the fraction of the volatiles released in-bed from the fines (X_{vf}), the conversion of gaseous volatiles in-bed (X_v), and the conversion in the bed of combustibles in devolatilized fines (X_{cf}) are determined. Also, the oxygen consumption rate in Region I (w_{ocli}) is calculated by mass balance. The parameter k_{oc}^* is adjusted until w_{oc} values converge. Then the iteration for \bar{C}_{ob} is performed until convergence. From the converged values for X_v , X_{cf} , and X_c , the total in-bed carbon conversion (X_{ic}) and in turn the in-bed combustion efficiency (E_{bc}) are computed.

Typical parameters for which the performance code requires input and their origin are indicated in Table 1.

VALIDATION

The objective is to validate the performance code for different AFBC unit sizes and fuel types. The code predictions for in-bed combustion of Kentucky No. 9 coal are compared with experimental data from 1 x 1 [B&W], 6 x 6 [EPRI/B&W], and 20 MW_e [TVA/EPRI] AFBC units in Figure 6. The data correspond to a gas residence time of about 0.5 second based on superficial velocity. Good agreement is observed. The in-bed combustion efficiency tends to decrease with an increase in feedpoint spacing but does not exhibit a smooth variation. The relatively high value obtained in the case of the 1 x 1 unit is due to lower gas velocity and lesser feed system attrition.

Figure 7 presents the results for Texas lignite. The square symbol stands for experimentally determined in-bed combustion efficiency and the solid line represents the code predictions. Experimental values of the overall combustion efficiency are also plotted for comparison. Predicted in-bed combustion and experimental overall combustion efficiency curves diverge with an increase in superficial gas velocity. This implies increased freeboard combustion at higher gas velocities. This is to be expected in view of the greater freeboard solids loading caused by CEMA, elutriation, and carry over of fines in the feed. Additional comparisons for Kentucky No. 9 and Pittsburgh No. 8 bituminous coals have been presented in a previous paper (3).

SENSITIVITY ANALYSIS

An analysis for sensitivity over the range of parameter uncertainty is desirable to further evaluate the code, identify the controlling parameters, and guide experimental work. The parameters which have significant impact on code predictions are anticipated to differ with AFBC unit size, design, and coal type. Therefore, a number of test analyses are required to generalize the results. Based on initial studies, the sensitivity of different parameters for burning Kentucky No. 9 coal in two different AFBC units (1 x 1/0.1 MW and 18 x 12/ 20 MW_e) are given in Table 2. Volatile conversion in-bed is typically complete (~100%) in the 1 x 1 AFBC unit and there-

fore its performance is primarily sensitive to char conversion parameters. VYULT impacts char fraction and hence is important. Due to the large feedpoint spacing in the 20 MW_g pilot plant, the parameter COFDO assumes a lead role. It is difficult to combust fines in a short residence time and consequently DHOP exerts a considerable influence on performance of both units.

SIMULATION

The response of the 20 MW_g pilot plant to changes in the fines content of the feed and feed system attrition coefficient are shown in Figure 8. COFATT of 11.0 corresponds to the extent of attrition that occurs in the current design. Clearly, it is beneficial to control the amount of fines in the feed and reduce feed system attrition. Results of additional simulations pertaining to the operation of the unit will be presented in another paper (12).

CONCLUSIONS

A phenomenological code for predicting in-bed combustion performance of AFBC units has been developed and validated. It provides a measure of required in-bed heat transfer surface allocation. Work is in progress to develop a freeboard combustion model. Future goals are to incorporate the effect of recycle and model overbed-feed mode and sulfur capture. The code is being tested and refined constantly based on new information and data. Upon completion, FBCSIM will become a versatile tool for performance simulation and design of fluidized-bed coal combustors.

ACKNOWLEDGMENT

This work was performed with the support of EPRI. We are thankful to N. Soltys and L. A. Oberjohn of B&W for their help in conducting the sensitivity analysis.

REFERENCES

1. Chandran, R.R., Duqum, J.N., Perna, M.A., Jafari, H.C., Rowley, D.R., Petrill, E.M., and Hansen, W.A., "A New Method for AFBC Fuels Characterization", 1987 International Conference on Fluidized Bed Combustion, The American Society of Mechanical Engineers, p. 292, 1987.
2. Chandran, R.R., Duqum, J.N., and Modrak, T.M., "Coal Classification for Fluidized Bed Combustion", International Symposium on Coal Combustion, Beijing, China, Sept. 1987 (to be published by Hemisphere Publ. Corp.)
3. Chandran, R.R., Duqum, J.N., and Petrill, E.M., "A Performance Code for AFBC Scaleup - Part I: In-Bed Combustion", 1987 International Conference on Fluidized Bed Combustion, The American Society of Mechanical Engineers, p. 300, 1987.
4. Bywater, R.J., "The Effects of Devolatilization Kinetics on the Injector Region of Fluidized Beds," 6th International Conference on FBC, Atlanta, GA, Conf. 800428, Vol. III, p. 1092, 1980.
5. Daw, C.S., "Tubular Flow Reactor Experiment - Task 13", Oak Ridge National Laboratory, Oak Ridge, TN, July 1985.
6. Burke, S.P. and Schumann, T.W.E., Ind. Eng. Chem., Vol 20, p. 998, 1928.
7. Levenspiel, O., Kunii, D., and Fitzgerald, T., Powder Technology, Vol. 2, p. 87, 1968/69.
8. Kunii, D. and Levenspiel, O., Fluidization Engineering, John Wiley & sons, Inc., New York, NY, 1969.
9. Overturf, B.W. and Kayihan, F., "Computations for Discrete Cut Particle Size Distributions in a Fluidized Bed Reactor", Powder Technology, Vol 23, p. 143, 1979.
10. D'Amore, M., Donsi, G., and Massimilla, L., "Bed Carbon Loading and Particle Size Distribution in Fluidized Combustion of Fuels of Various Reactivity," 6th International Conference on FBC, Atlanta, GA, Conf-800428, Vol. I, p. 675, 1980.

11. Beer, J.M., Massimilla, L., and Sarofim, A.F., Inst. Energy Symposium Series 4: Fluidized Combustion, Systems and Applications, p. IV.5.1, 1980.
12. Divilio, R. J., Towers, T.A., and Chandran, R.R., "Applications of FBCBAL and B&W Combustion Model to the EPRI AFBC Demonstration Programs", 1988 EPRI Seminar, Palo Alto, CA, May 3-5, 1988 (to be presented).

TABLE 1. PERFORMANCE CODE INPUT DATA

<u>Model Input Parameter</u>	<u>Description</u>	<u>Source</u>
Unit cell cross section Feedpoint location Bed temperature Coal feed rate Bed height Transport air Primary air Bed material density Bed weight Freeboard cross section Bed material size distribution Coal size distribution at the hopper	Operating conditions	Validation test conditions or design specifications
Coal composition Coal density Higher heating value	Coal properties	ASTM procedures
Coal attrition parameters	FSATT subroutine	Feed System attrition tests
Gas dispersion coefficient Solids velocity Solids dispersion coefficient Entrainment rate coefficient	Hydrodynamics module	Literature
Coal particle heatup time Volatile yield Devolatilization rate constant Volatile composition Char fraction Char reactivity Char composition	Chemical kinetics module	Fixed bed reactor
Swelling index Fragmentation index	Chemical kinetics module	Bench-scale AFBC unit
CEMA rate constant Weight fraction of flakes	Solids distribution module	Bench-scale AFBC unit

TABLE 2. SENSITIVITY ANALYSIS

Parameter	Type	Description	Sensitivity	
			1 x 1 B&W	20 MW _g TVA
DBED	Operational	Bed material mean size	Negl	Negl
DHOP	Operational	Coal feed size distribution	High	High
COFATT	Un _{it} /Fuel	Feed system attrition coeff	Medium	High
ATTEXP	Un _{it} /Fuel	Feed system attrition exponent	Medium	High
COFUSC	Hydrodynamic	Coarse particle velocity coeff	Medium	Medium
COFOSC	"	Coarse particle dispersion coeff	Low	Medium
COFOD	"	Gas dispersion coeff	Low	High
COFUSF	"	Fines velocity coeff	Low	Low
COFOSF	"	Fines dispersion coeff	Low	Low
COFOE	"	Entrainment rate coeff	High	Medium
FRFLAK	Fuel	Weight fraction of CEMA flakes	Negl	Low
KCAN	"	CEMA rate constant	Low	Low
COFTAU	"	Coal particle heat-up time coeff	Negl	Medium
VYULT	"	Ultimate volatile yield	High	Low
COFFVY	"	Volatile yield coeff	Negl	Negl
COFVR	"	Devolatilization rate coeff	Low	Medium
KVEXP	"	Devolatilization rate exponent	Low	Low
SIULT	"	Swelling index upper limit	Low	Low
COFRCC/ RCCACT	"	Char reactivity (Pre-exponential factor/activation energy)	High	High
E _{ibc} Range (%)			68 - 91	63 - 85

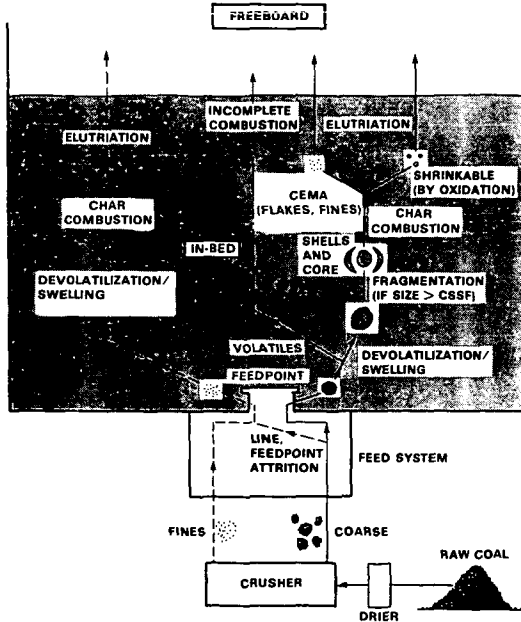


Figure 1. Coal combustion sequence for underbed feed.

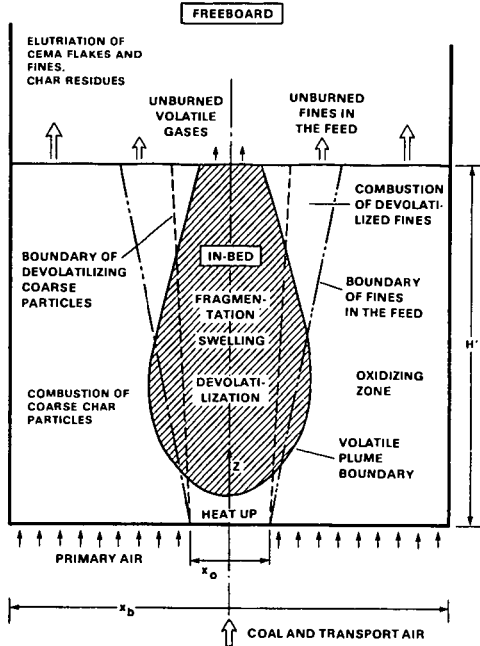


Figure 2. Conceptual model of in-bed combustion.

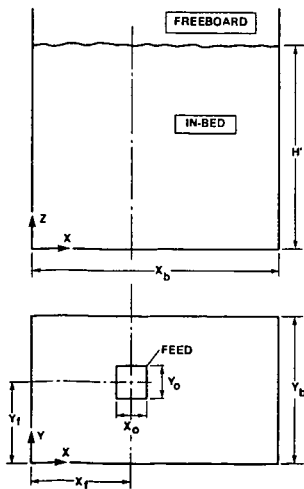


Figure 3. Unit cell coordinate geometry.

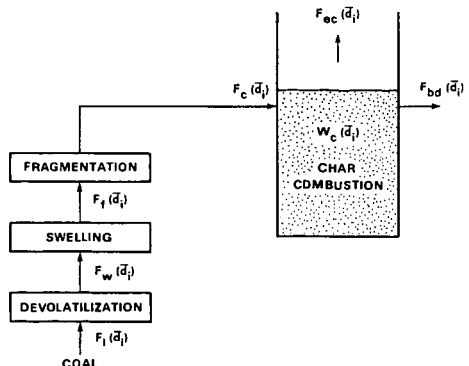


Figure 4. Flow rates pertaining to different steps of the combustion sequence - Region II model.

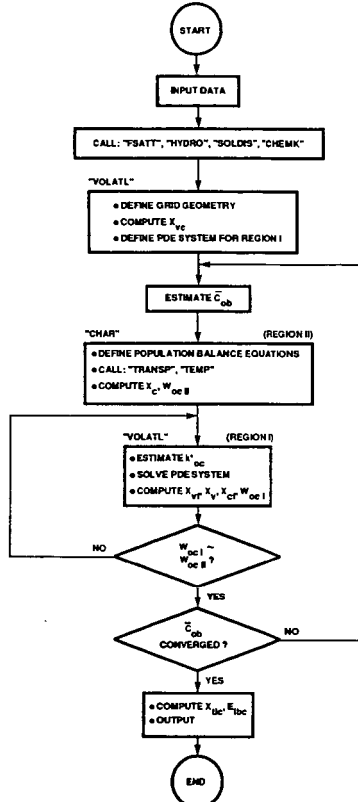


Figure 5. Performance code flowchart.

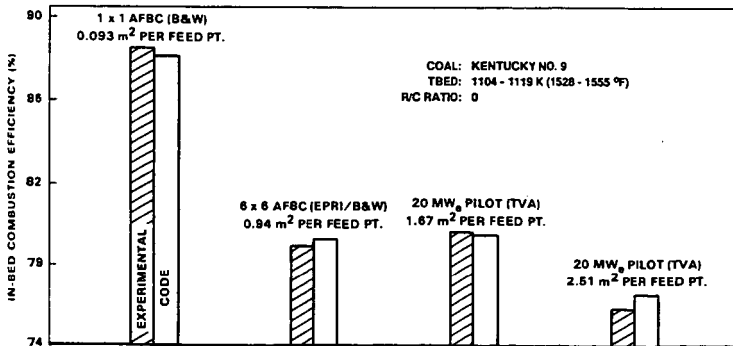


Figure 6. Comparison of performance code predictions with experimental data.

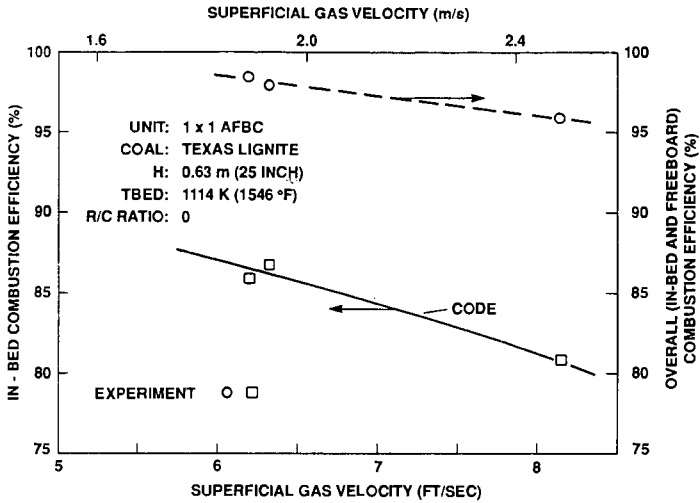


Figure 7. Comparison of code predictions with data.

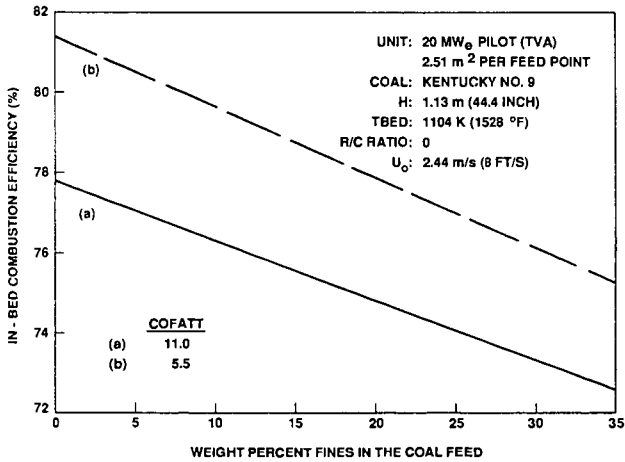


Figure 8. Simulation for coal hopper particle size distribution.